Permutationally invariant fitting of intermolecular potential energy surfaces: A case study of the Ne-C_2H_2 system

Jun Li, and Hua Guo

Citation: The Journal of Chemical Physics **143**, 214304 (2015); doi: 10.1063/1.4936660
View online: https://doi.org/10.1063/1.4936660
View Table of Contents: http://aip.scitation.org/toc/jcp/143/21
Published by the American Institute of Physics

Permutationally invariant fitting of intermolecular potential energy surfaces: A case study of the Ne-C_2H_2 system

Jun Li[1,a)] and Hua Guo[2]
[1]*School of Chemistry and Chemical Engineering, Chongqing University, Chongqing 400044, China*
[2]*Department of Chemistry and Chemical Biology, University of New Mexico, Albuquerque, New Mexico 87131, USA*

(Received 30 September 2015; accepted 16 November 2015; published online 2 December 2015)

The permutation invariant polynomial-neural network (PIP-NN) approach is extended to fit intermolecular potential energy surfaces (PESs). Specifically, three PESs were constructed for the Ne-C_2H_2 system. PES1 is a full nine-dimensional PIP-NN PES directly fitted to ~42 000 *ab initio* points calculated at the level of CCSD(T)-F12a/cc-pCVTZ-F12, while the other two consist of the six-dimensional PES for C_2H_2 [H. Han, A. Li, and H. Guo, J. Chem. Phys. **141**, 244312 (2014)] and an intermolecular PES represented in either the PIP (PES2) or PIP-NN (PES3) form. The comparison of fitting errors and their distributions, one-dimensional cuts and two-dimensional contour plots of the PESs, as well as classical trajectory collisional energy transfer dynamics calculations shows that the three PESs are very similar. We conclude that full-dimensional PESs for non-covalent interacting molecular systems can be constructed efficiently and accurately by the PIP-NN approach for both the constituent molecules and intermolecular parts. © *2015 AIP Publishing LLC.* [http://dx.doi.org/10.1063/1.4936660]

I. INTRODUCTION

Energy transfer almost always accompanies gas phase collisional processes, whether reactive or non-reactive. As a result, it is of great significance in many fields, such as reaction kinetics, relaxation of excited molecules, spectroscopy, and so on.[1–4] In chemical reactions, for example, reactant molecules might gain energy via collisions with the surrounding species to surmount the reaction barrier, and product molecules might lose energy in collisions to become stabilized. Furthermore, collisional energy transfer with reaction intermediates plays a key role in kinetics. As a result, a quantitatively accurate understanding of these processes is essential and the energy transfer rates might have to be included in modeling kinetics of reactions, particularly those with a pressure dependence, as done in master equation-based approaches.[3,5]

Theoretically, the energy transfer dynamics, like any other collisional processes, can often be considered on an adiabatic potential energy surface (PES), according to the Born-Oppenheimer approximation. Once the PES is known, scattering properties can be determined, at least, in principle, with various types of dynamical theories, such as quasi-classical trajectory (QCT) and quantum scattering methods. Consequently, an accurate PES is highly desired for these dynamical studies. Unfortunately, there are presently few high-quality PESs for studying energy transfer. As pointed out recently by Jasper *et al.*[6] and Conte *et al.*,[7] the PES is often a significant source of error in simulating collisional energy transfer. An alternative to developing PESs for energy transfer is Born-Oppenheimer direct dynamics,[8] in which the forces are computed on the fly. However, this approach may suffer from high computational expenses if high-level *ab initio* electronic calculations or long time propagation are needed.

For rotational energy transfer problems, the molecules can be reasonably treated as rigid bodies. As a result, the interaction PES between the two colliding partners only needs to involve the intermolecular degrees of freedom. On the other hand, if vibrational energy transfer is important, all internal degrees of freedom are required.[9–11] However, the fit of the entire PES with all intra- and inter-molecular coordinates using a single function is neither numerically efficient nor physically necessary. Indeed, the PES has traditionally been expressed as a sum of the intramolecular PES and its intermolecular counterpart describing the interaction between the two colliders, with the latter approximated by a sum of pairwise functions dependent on the interatomic distances.

The intramolecular PESs can now be accurately fit to *ab initio* data points using many methods, including spline,[12] many-body expansion (MBE),[13,14] reproducing kernel Hilbert space (RKHS),[15] modified Shepard interpolation (MSI),[16,17] interpolating moving least squares (IMLS),[18,19] permutation invariant polynomial (PIP),[20,21] neural network (NN),[22–24] and PIP-NN methods.[25,26] The recently proposed PIP-NN approach has some unique advantages: it is highly faithful, rigorous, and general in enforcing the permutation invariance in the PES, simple to implement, and computationally efficient. Its applications in various systems have demonstrated its efficiency and accuracy.[27–30] We note in passing that the accuracy of the intramolecular PES may not be critical to the average energy transfer but may affect rare events such as supercollisions.[7]

The intermolecular PES typically has attraction and repulsion parts. The accuracy of the energy transfer dynamics

a)Author to whom correspondence should be addressed. Electronic mail: jli15@cqu.edu.edu

is largely determined by the repulsive walls.[10,31] However, an accurate description of the attractive part of the intermolecular PES is also desirable as it may play an important role in low-temperature collisions and with large impact parameters.[32] Several simplified pairwise functional forms have been suggested and tested for intermolecular PESs, including Lennard-Jones and its modifications,[33] Buckingham,[34] Varandas,[35,36] and Tang-Toennies.[37] Recently, Jasper *et al.* tested the Lennard-Jones and modified Buckingham potential functions against full-dimensional direct dynamics calculations and concluded that these simplified analytical pairwise functional forms may introduce errors for systems with significantly anisotropic intermolecular interactions,[38] presumably due to many-body interactions. Bowman and his co-workers applied the PIP approach with full permutational symmetry to non-covalent interactions in several systems including $(H_2O)_2$[39] and $(H_2O)_3$,[40] $(HCl)_2$,[41] $(HCl)_3$,[42] and mixed HCl-H_2O clusters.[43] Importantly, this approach does not rely on the pairwise assumption and contains many-body terms. Later, Truhlar and co-workers pointed out that a single polynomial representation does not separate into non-interacting fragments and proposed a remedy by removing a small number of basis functions that do not rigorously separate.[44] Bowman and co-workers called such a partially permutationally invariant basis "purified invariant polynomial basis,"[45] which does not allow exchange of identical atoms from different fragments. These new approaches are accurate and faster to evaluate, in addition to permutation symmetry, and the resulting PESs provide a better description of the interaction in the asymptotic limit. These advantages make these methods suitable for multi-component systems, where the fitting and evaluation are unnecessary and too demanding if the full-permutation-invariant basis is used. By using the reduced bases, the fitting errors for the intermolecular PES of the systems Ar-HOCO, CH_4-H_2O, and CH_4-H_2O-H_2O have been found to be all quite small.[45–47]

In this work, we extend our PIP-NN approach to fit the interaction PES, with the system Ne-C_2H_2 as an application. This C_2H_2 system involves two isomers, namely, acetylene (HCCH) and vinylidene (H_2CC). While the collision induced relaxation of vibrationally excited C_2H_2 has been extensively studied by Smith, Dai, and co-workers,[48,49] few theoretical investigations have been performed. In Section II, PESs of the Ne-C_2H_2 system are presented using three different methods. The first approach is a PIP-NN fit of the entire system without separating the PES into the intramolecular and intermolecular parts. This PES (PES1) is fitted to ca. 42 000 *ab initio* energies and served as a benchmark. In the second and third cases, the PESs are both expressed as a sum of the C_2H_2 PES and interaction PES between C_2H_2 and Ne. The intramolecular PIP-NN PES for C_2H_2 is adopted from our recent work,[50] which has been validated by energy level calculations of both the acetylene and vinylidene isomers.[50,51] For the intermolecular PES, two approaches are employed, both using the purified PIPs. PES2 is a PIP fitting while PES3 is obtained using the PIP-NN method. In Section III, results on the three PESs are compared and discussed. Collisional energy transfer is simulated using a classical trajectory method and the preliminary results are presented in Section IV. Conclusions and final remarks are given in Section V.

II. POTENTIAL ENERGY SURFACES

A. *Ab initio* calculations

The *ab initio* points used in the fits include nearly ~20 000 points for various C_2H_2 geometries with the Ne atom about 8 Å away from the center of mass of C_2H_2 in order to provide the correct collisional asymptote. An additional set of geometries was generated with Ne closer to C_2H_2 by running direct dynamics at a low level of theory, B3LYP/6−31+G(d). Based on these points, a primitive PES was generated. Classical trajectories with various initial conditions were then propagated on the PES to explore the configuration space and improve the PES by adding new points in regions with large fitting errors. Note that the new points were screened to remove geometries that are too close to each other.[28] This procedure was iterated several times until the results were converged. Finally, about 42 000 points were calculated using the explicitly correlated coupled cluster with singles, doubles, and perturbative triples (CCSD(T)-F12a) method[52,53] with the correlation-consistent triple-ζ basis set optimized for describing core-valence correlation effects with the explicitly correlated method (cc-pCVTZ-F12),[54] which has been used for developing C_2H_2 PES. The MOLPRO suite of electronic structure programs[55] was used in all *ab initio* calculations.

B. PES1

This PES for the C_2H_2-Ne system was constructed directly using the PIP-NN method,[25,26] without separating the intramolecular and intermolecular terms. Since details of the PIP-NN fitting method have been extensively discussed in our previous work,[25,26] only a brief description is given here. Explicitly, the nine-dimensional (9D) PES was fit using the following functional form, represented by a feed-forward NN with two hidden layers:

$$V = b_1^{(3)} + \sum_{k=1}^{K} \left(\omega_{1,k}^{(3)} \cdot f_2 \left(b_k^{(2)} + \sum_{j=1}^{J} \left(\omega_{k,j}^{(2)} \cdot f_1 \left(b_j^{(1)} + \sum_{i=1}^{I} \omega_{j,i}^{(1)} \cdot G_i \right) \right) \right) \right), \quad (1)$$

where J and K are the number of the neurons of the two hidden layers, respectively; f_i is the transfer function taken as the hyperbolic tangent function; $\omega_{j,i}^{(l)}$ are weights that connect the ith neuron of $(l-1)$th layer and the jth neuron of the lth layer; $b_j^{(l)}$ are biases of the jth neurons of the lth layer. The major difference from a conventional NN approach is

that the input layer of the NN is replaced by low-order PIPs, $G_i = \hat{S}\prod_{j<k}^{N} p_{jk}^{l_{jk}}$, rather than the coordinates. The use of the PIPs rigorously enforces the permutation invariance of the PES. I denotes the number of permutation invariant polynomials G_i of the input layer, namely, $G_i = \hat{S}\prod_{j<k}^{N} p_{jk}^{l_{jk}}$, see also below; similar to our previous work on the CH_2OO PES,[28] which is an A_2B_2C molecule as in the current system, PIPs up to the third order ($I = 101$) were used. The resulting PES is denoted as PES1 and served as a benchmark for other forms of PESs discussed below.

C. PES2

In the second approach, the PES is expressed as

$$V_{\text{Ne-C}_2\text{H}_2} = V_{\text{intra}} + V_{\text{inter}}, \tag{2}$$

where V_{intra} is the isolated 6D PIP-NN PES for C_2H_2 and V_{inter} is the interaction PES between Ne and C_2H_2. For each of the 42 000 *ab initio* geometries, the interaction PES can be easily obtained by $V_{\text{inter}} = V_{\text{Ne-C}_2\text{H}_2} - V_{\text{intra}}$, where $V_{\text{Ne-C}_2\text{H}_2}$ is PES1 and V_{intra} is the isolated PES for C_2H_2 reported in our recent work.[50] In other words, the target energy at these geometries used in the fitting is that of the potential difference, rather than the *ab initio* value itself. This is a reasonable approximation that is sufficient here for us to test and compare the fitting methods, because both the C_2H_2 PES and PES1 for the Ne-C_2H_2 system are accurate.

Instead of using a pairwise form to approximate V_{inter}, as done in many previous studies, we represent this 9D term using the PIP method but with two reduced bases, as suggested by Bowman *et al.*[45] To define the PIP basis used in the fitting of the intermolecular PES, let us first examine the PIP approach to fit the entire PES,

$$V_{\text{Ne-C}_2\text{H}_2} = V\left(\hat{S}\prod_{i<j}^{N} p_{ij}^{l_{ij}}\right), \tag{3}$$

where $\hat{S}$ is the symmetrization operator, which consists of all possible relevant nuclear permutation operations in the system, $p_{ij} = \exp(-\alpha r_{ij})$ are the Morse-like variables with α as an adjustable constant and r_{ij} the $N(N-1)/2$ (here $N = 5$) internuclear distances. l_{ij} is the degree of p_{ij} and $M = \sum_{i<j}^{N} l_{ij}$ is the total degree in each monomial.

If the atoms in Ne-C_2H_2 are denoted in the following order: H(1)H(2)C(3)C(4)Ne(5), then explicitly, the monomials of Eq. (3) are expressed as

$$p_{12}^{l_{12}} p_{13}^{l_{13}} p_{14}^{l_{14}} p_{15}^{l_{15}} p_{23}^{l_{23}} p_{24}^{l_{24}} p_{25}^{l_{25}} p_{34}^{l_{34}} p_{35}^{l_{35}} p_{45}^{l_{45}}. \tag{4}$$

Since the 6D C_2H_2 PES (V_{intra}) is independent of any distances involving Ne, it is clear that V_{intra} needs to satisfy the condition: $l_{15} = l_{25} = l_{35} = l_{45} = 0$, i.e., $l_{i5} = 0$ (i = 1–4). Apparently, the remaining terms in Eq. (4), namely, those with $\sum_i l_{i5} \neq 0$, must be considered in the 9D interaction PES (V_{inter}). In this way, the entire PES for the C_2H_2-Ne system can be exactly separated into two parts, V_{intra} and V_{inter} without approximation, as shown in Eq. (5). One can see that both of the PES parts are functions of the PIPs, which enforce the relevant permutation symmetry in the PESs,

$$\begin{aligned} V_{\text{Ne-C}_2\text{H}_2} &= V\left(\hat{S}\prod_{i<j}^{N} p_{ij}^{l_{ij}}\right) \\ &= V_{\text{C}_2\text{H}_2}\left(\hat{S}\prod_{i<j, l_{i5}=0}^{N} p_{ij}^{l_{ij}}\right) + V_{\text{inter}}\left(\hat{S}\prod_{i<j, \sum_i l_{i5}\neq 0}^{N} p_{ij}^{l_{ij}}\right). \end{aligned} \tag{5}$$

Here, two different PIP bases were used. The first includes all PIPs with the condition, $\sum_i l_{i5} \neq 0$, which corresponds to what Conte *et al.* denoted as "purified basis."[45] This basis can be further reduced by assuming that V_{inter} is only dependent on r_{i5} (i = 1–4), the distances between Ne and the atoms in C_2H_2. This corresponds to the "pruned purified basis" defined by the same authors,[45] with $l_{12} = l_{13} = l_{14} = l_{23} = l_{24} = l_{34} = 0$, or $l_{ij} = 0$ ($i < j$ and i, j = 1–4). Although the number of PIPs is greatly reduced in this basis, it might introduce significant errors, since this rather crude approximation does not recognize the internal conformation of C_2H_2. The two PESs obtained with these two bases are denoted as PES2 (purified bases) and PES2′ (pruned purified bases), respectively. The "purification" discussed above differs somewhat from the numerical way proposed by Bowman and co-workers,[45] but they achieve the same results. The "purification" methods can be easily generalized. For instance, for the non-covalent H_2O-H_2 system in which the atoms are ordered as [H(1)H(2)O(5)][H(3)H(4)], the intramolecular PES for H_2O depends only on the internuclear distances r_{12}, r_{15}, and r_{25}, requiring $l_{i3} = l_{i4} = 0$ (i = 1, 2, 5), and $l_{34} = 0$, while the H_2 PES depends on r_{34}, requiring all other powers equal to zero. The remaining terms can thus be included for fitting the interaction PES. The restriction in such a PES is that the hydrogen interchanges between H_2O and H_2 are not allowed.

D. PES3

The PIPs can be used directly as a basis to fit the *ab initio* points, as done by Bowman and co-workers.[39–43] They can also be used as symmetry functions to enforce permutation symmetry in NN fitting, as in the PIP-NN method.[25,26] Therefore, the PIP-NN approach can be extended in a straightforward fashion to fit V_{inter}. In this third approach, the main idea is similar to the original PIP-NN method,[25,26] namely, the input layer is replaced by low-order PIPs. The only distinction is that the fitting of the intermolecular PES involves only those PIPs that satisfy the constraint $\sum_i l_{i5} \neq 0$. The NN fitting was done using the same protocol as described in Sec. II B. The PES constructed by this method is denoted as PES3. Here, we did not try the pruned purified basis in the PIP-NN fitting.

III. RESULTS AND DISCUSSION

In fitting PES1, several different NN structures were tested. The final PIP-NN PES employed an NN with two

TABLE I. Maximum degrees (M), number of the parameters (No.), RMSE (in meV), and MAD (in meV) for different PESs. Note that PES1 is for the whole system, and others are for the intermolecular interaction. PES1 and PES3 are fitted by PIP-NN with full and purified bases, respectively. PES2 and PES2′ are fitted by PIP with purified and pruned purified bases, respectively.

	M	No.	RMSE	MAD
PES1	3	2891	1.09	45.55
PES2	4	248	12.18	864.67
	5	751	3.26	102.42
	6	2013	1.32	35.14
PES2′	4	30	26.94	945.40
	5	50	21.46	927.67
	6	80	19.71	1018.72
PES3	3	821	1.96	81.98

hidden layers with, respectively, 15 and 80 neurons (J = 15, K = 80), resulting in 2891 parameters. The final overall root mean square error (RMSE) is 1.09 meV with the maximum deviation (MAD) of 45.55 meV, as shown in Table I. The fitting errors are presented in Figure 1 along with their distributions. One can see that the small errors are evenly distributed in the energy range of 0–9 eV. The distributions of the fitting errors are also presented in the lower panel of Figure 1: ∼17 000 points have fitting errors less than 0.2 meV, ∼10 000 points within 0.2-0.4 meV, and ∼5000 points within 0.4-0.6 meV. The level of fitting accuracy is comparable to that of the PIP-NN PES of isolated C_2H_2, where the RMSE is 1.18 meV.[50]

Let us now turn to PES2 and PES2′, using the PIP method with reduced bases. As shown in Table I, the RMSE and MAD are listed for different maximum orders (M) of the PIPs for both the purified (PES2) and pruned purified bases (PES2′). In the former case, the RMSE and MAD all decrease significantly with M: 12.18, 3.26, and 1.32 meV, and 864.67, 102.42, and 35.14 meV, respectively, for M = 4, 5, and 6. Interestingly, the maximum order of the PIPs does not affect the fitting performance much with the pruned purified basis. As a result, this basis is capable of giving a relatively reasonable PES with low computational costs, especially for multi-component systems, as found in the work of Bowman *et al.*[45–47] Figure 2 presents the fitting errors as a function of the target energy (obtained by $V_{\text{inter}} = V_{\text{Ne-C}_2\text{H}_2} - V_{\text{intra}}$) for the most accurate PES2, namely, with M = 6 with 2013 coefficients (this PES will thereafter be referred to as PES2). The population of the fitting errors is also shown in Figure 2: most are rather small, as expected. It is worth noting that the basis set superposition error (BSSE) is not taken into account in our fittings, an issue to be discussed below.

As discussed above, the same data set has also been fit with the PIP-NN method, denoted as PES3. After several testing, the final version uses 69 PIPs (up to the third order) in the input layers and the number of neurons in each hidden layer was 10. As shown in Table I, the performance of PES3 is also excellent: its RMSE is 1.96 meV, comparable to the RMSE of 1.32 meV of PES2. Since this PIP-NN PES has only 821 fitting parameters, PES3 is about three times faster than PES2, which has 2013 fitting coefficients. Figure 2 presents the fitting errors and their distributions of PES3, which are quite similar to those of PES2.

In Figure 3, we compare several one-dimensional (1D) cuts for the interaction of Ne with acetylene (HCCH at its equilibrium geometry) for the three fitted PESs. The right

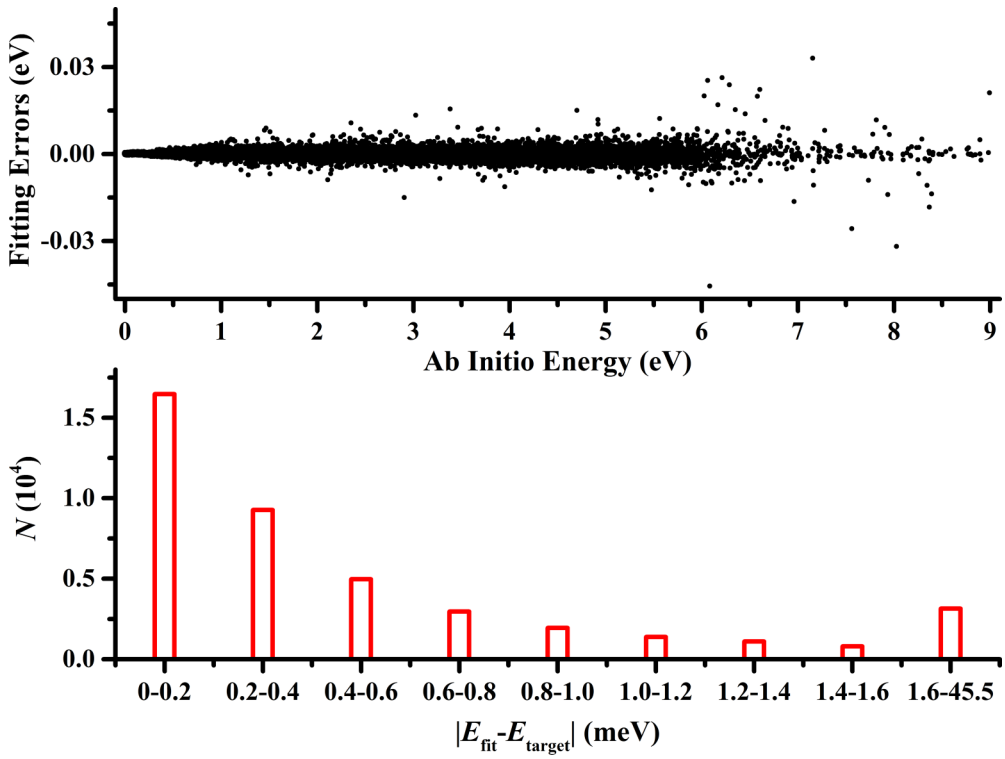

FIG. 1. Upper panel: fitting errors for the full-dimensional PIP-NN PES (PES1) as a function of the energy (in eV, relative to the Ne + acetylene (HCCH) asymptote); lower panel: distributions of fitting errors (defined as $|E_{\text{fit}} - E_{\text{target}}|$) for the PES1.

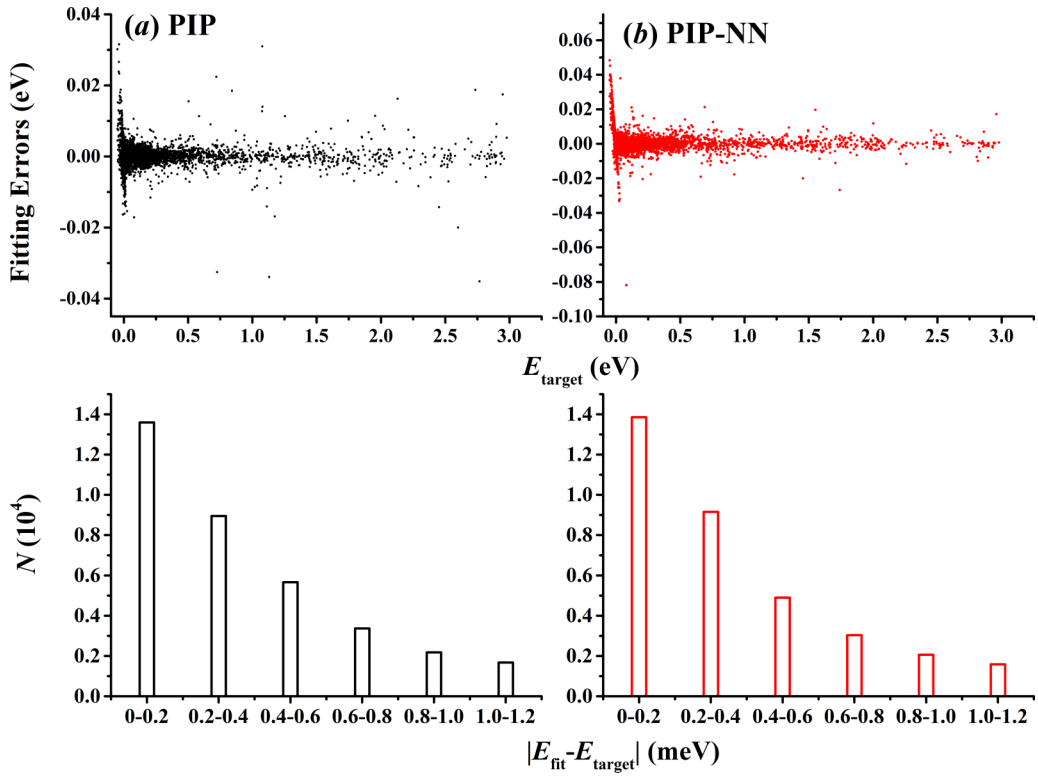

FIG. 2. Fitting errors for the PIP PES ((a) PES2) and the PIP-NN PES ((b) PES3) of the intermolecular interaction as a function of the target energy (in eV, relative to the Ne + HCCH asymptote); the distributions of their fitting errors (defined as $|E_{\rm fit} - E_{\rm target}|$) are also shown in the lower panel.

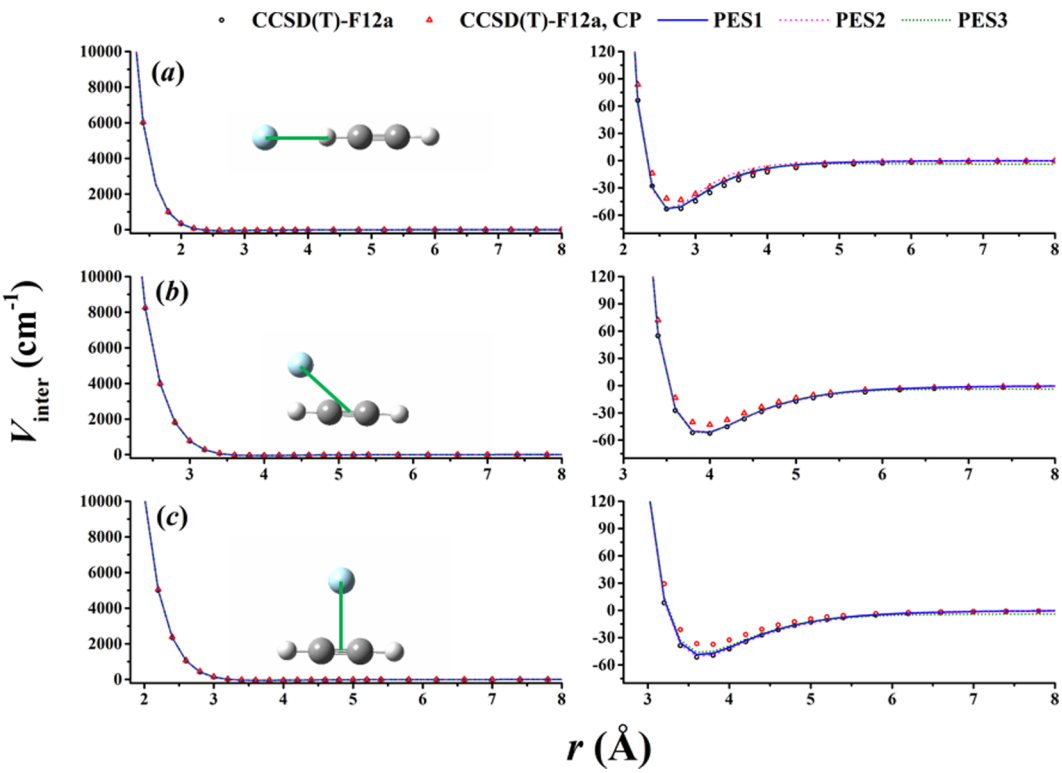

FIG. 3. Comparison of several 1D cuts for the interaction energy between HCCH (fixed at equilibrium) and Ne: CCSD(T)-F12a for CCSD(T)-F12a/cc-pCVTZ-F12 without BSSE, CP for counterpoise correction to correct the BSSE, and the PESs are as defined in the text. The energy is in cm^{-1} relative to the Ne + HCCH asymptote. The corresponding x-axis, (a) the inter-nuclear distance between Ne and H, (b) and (c) the distance between Ne and the center of mass of HCCH are displayed by the solid green line in the atomic configurations with HCCH fixed at its equilibrium. The left three panels are for the energy up to 10 000 cm^{-1}, while the right three panels show the details of the interaction below 120 cm^{-1}.

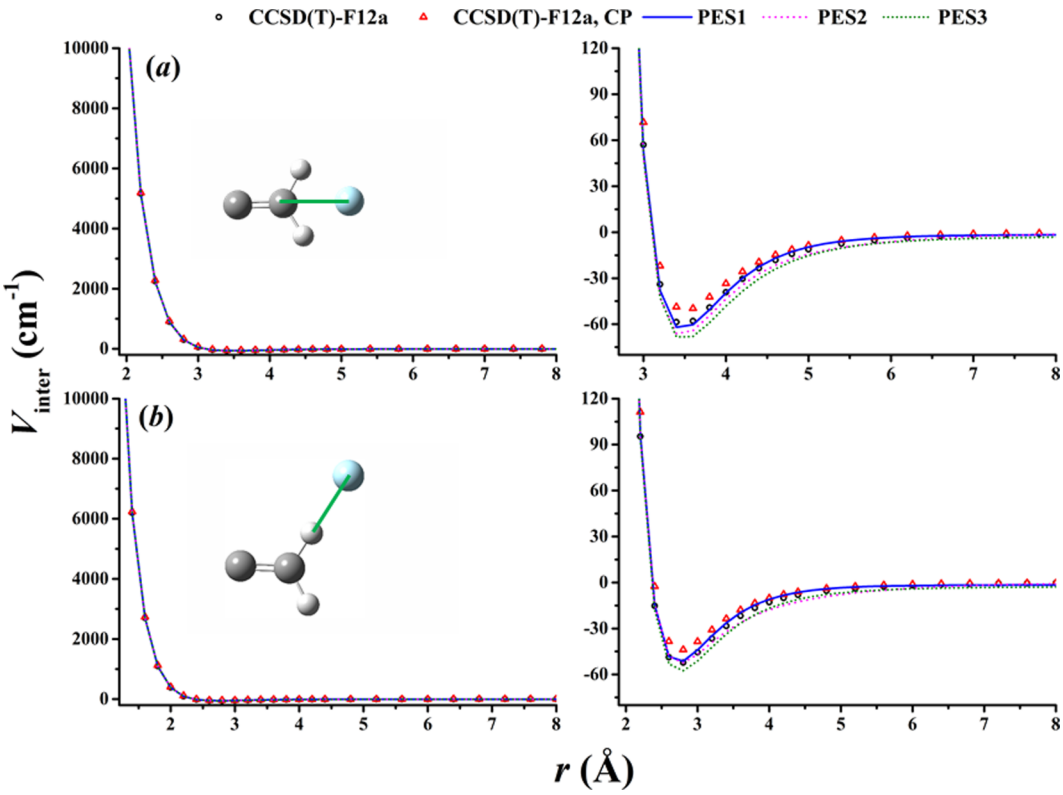

FIG. 4. Same as Figure 3, but for the interaction energy between H_2CC (fixed at equilibrium) and Ne. The energy is in cm^{-1} relative to the Ne + H_2CC asymptote. The corresponding x-axis is displayed by the solid green line in the atomic configurations with H_2CC fixed at its equilibrium.

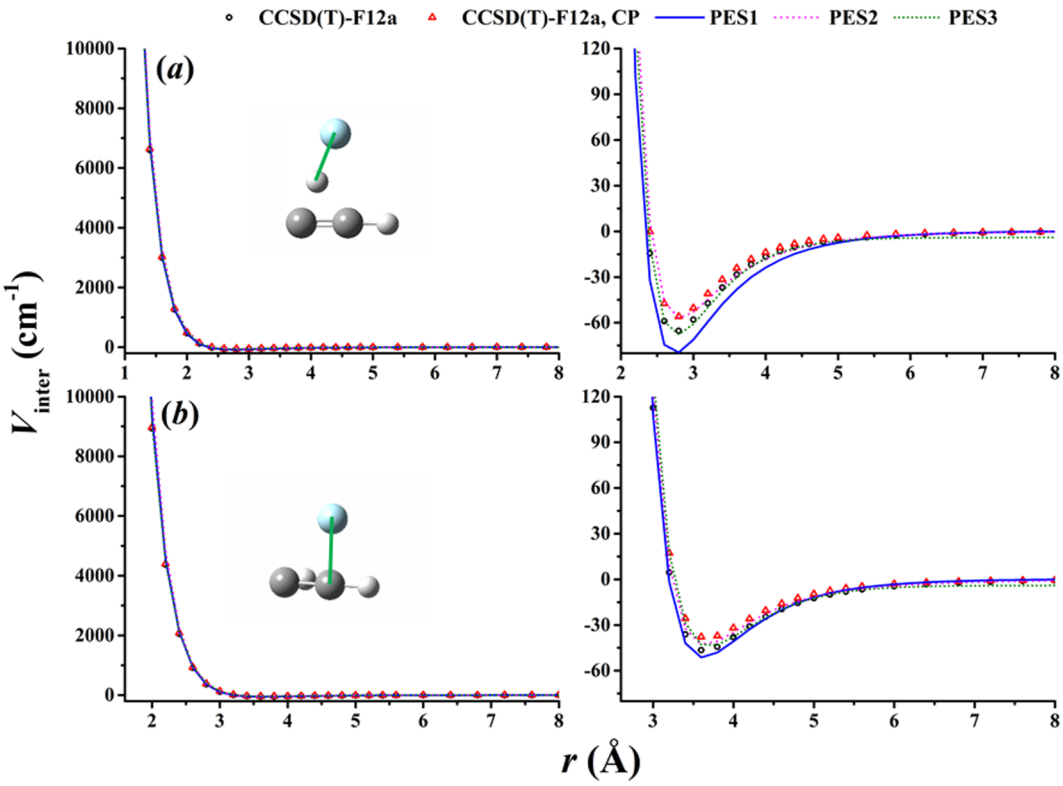

FIG. 5. Same as Figure 3, but for the interaction energy between HCCH-H_2CC isomerization transition state (TS2) and Ne. The energy is in cm^{-1} relative to the Ne + TS2 asymptote. The corresponding x-axis is displayed by the solid green line in the atomic configurations with TS2 fixed at its equilibrium. Note that the *ab initio* points were not included in the fitting.

column of the figure provides a closer comparison for the attractive region of the PESs. The agreement among them is quite satisfactory. Similarly, two 1D cuts for the interaction between Ne and vinylidene (H_2CC at its equilibrium geometry) are compared in Figure 4. PES3 shows a slightly deeper well than others, but the difference is on the order of at most 10 cm^{-1}. Other regions including the repulsive wall and asymptote are all well reproduced. Figure 5 presents two 1D cuts for the interaction between Ne and TS2, which corresponds to the transition state of the acetylene-vinylidene isomerization.[50] Unlike Figures 3 and 4, the data in Figure 5 were not included in the fitting. It can be seen that the performance of each PES is comparable, although **PES1** possesses a slightly deeper well, while **PES2** shows a shallower one.

As mentioned above, the effects of BSSE were not considered in this work, because we are focusing on the fitting aspects of the PES. However, the BSSE can be significant and it needs to be corrected if an accurate representation of the interaction PES is to be constructed. To give some idea about the effects of BSSE in this system, we also compare the PESs in Figures 3-5 with two sets of *ab initio* points at the level of CCSD(T)-F12a/cc-pCVTZ-F12 with or without BSSE. The Boys and Bernardi counterpoise correction[56] was used to correct for BSSE. One can see that all PESs reproduce the *ab initio* values reasonably well, both for the repulsive walls up to 10 000 cm^{-1}, the interaction region, and the asymptotic limit. The BSSE is quite small and mostly in the attractive regions, but it is non-negligible.

Figures 6 and 7 present the comparison of the two-dimensional (2D) interaction PESs for Ne-HCCH and Ne-H_2CC, respectively. Both target molecules HCCH and H_2CC were fixed at their respective equilibrium geometries and placed with their configurations showed in the same figures, with the Ne atom approaches the target molecule within the YZ plane. It is apparent that all three PESs are all quite similar to each other.

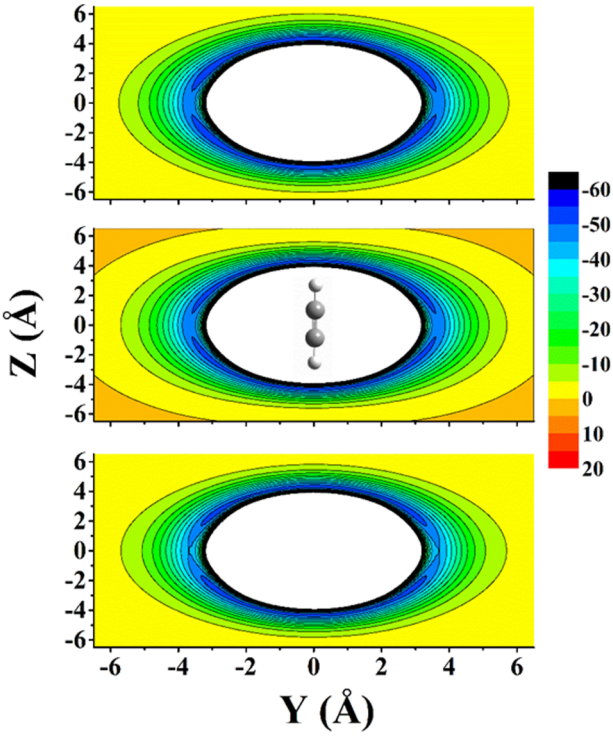

FIG. 6. Contour plots of the intermolecular potential of PES1, PES2, and PES3 (from top to bottom) with HCCH fixed at the equilibrium structure along the Z axis. Ne approaches HCCH within the YZ plane. The energies are in cm^{-1} relative to the Ne + HCCH asymptote with an interval of 5 cm^{-1}.

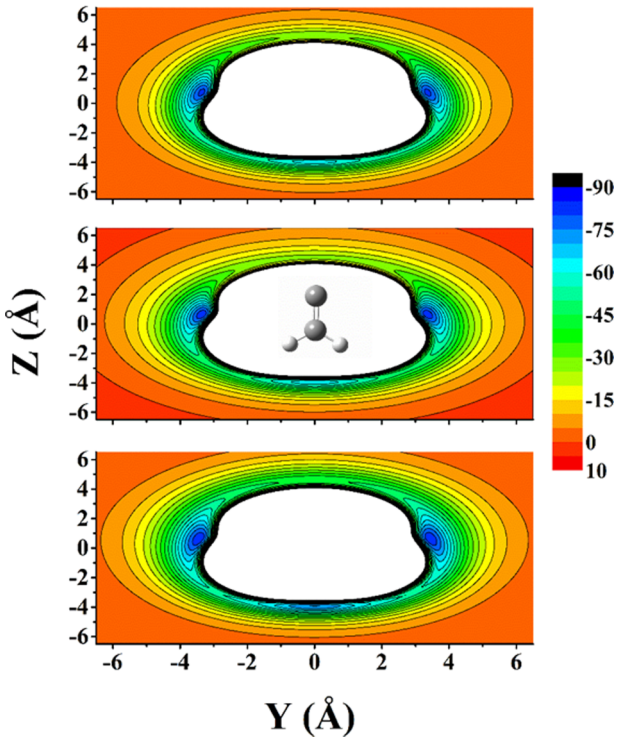

FIG. 7. Contour plots of the intermolecular potential of PES1, PES2, and PES3 (from top to bottom) with H_2CC fixed at the equilibrium structure. Ne approaches H_2CC within the YZ plane. The energies are in cm^{-1} relative to the Ne + H_2CC asymptote with an interval of 5 cm^{-1}.

IV. COLLISIONAL ENERGY TRANSFER DYNAMICS

To test the PESs in studying energy transfer dynamics, standard classical trajectory calculations were performed using VENUS.[57] The initial total vibrational energy of the non-rotating HCCH was set to 45 kcal/mol including the zero-point energy, with the translational energy between Ne and HCCH being 5 kcal/mol. The internal energy of HCCH is slightly higher than the isomerization barrier. The initial vibrational energy of each normal mode is determined randomly using the harmonic oscillator approximation at constant total vibrational energy of HCCH. Once the normal mode energy is specified, the initial coordinates and momenta of the normal mode are chosen by the microcanonical sampling technique.[58] The trajectories were initiated with a separation of 8.0 Å and terminated when they are separated by 8.0 Å. The impact parameter b was scanned from 0.0 to 5.0 Å with a step size of 0.5 Å. At each b, 10^4 trajectories were propagated. The gradient of the PES is obtained numerically by a central-difference algorithm with the propagation time step 0.01 fs. All trajectories conserved energy within a chosen criteria (10^{-4} kcal/mol). Figure 8 presents the b-dependent average unsigned

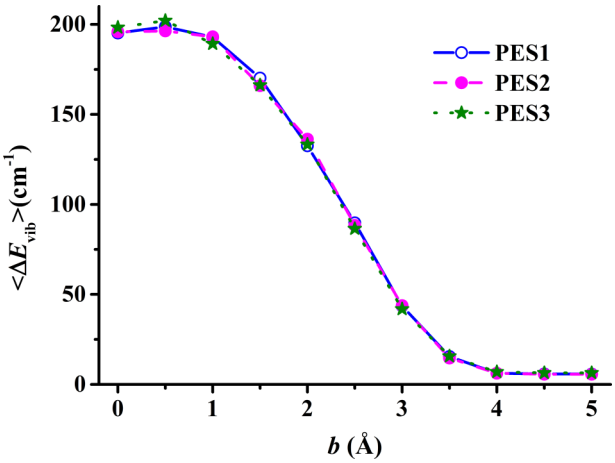

FIG. 8. The b-dependent average unsigned vibrational energy transfer $\langle \Delta E_{\rm vib} \rangle$ on the three PESs for Ne + HCCH with an initial vibrational energy of 45 kcal/mol (including the zero point vibrational energy) and collision energy of 5 kcal/mol.

vibrational energy transfer on the three PESs according to

$$\langle \Delta E_{\rm vib} \rangle_{\rm unsign} = \sum_j \left| E_{{\rm vib},f} - E_{{\rm vib},i} \right| / N, \qquad (6)$$

where the subscripts "i" and "f" denote "initial" and "final," respectively. As expected, the results are all in good agreement with each other, indicating that the three PESs provide essentially the same characterization of the interaction potential. More detailed QCT calculations will be reported in a subsequent publication.

V. CONCLUSIONS

PESs are central to various dynamical and spectroscopic studies in the field of chemistry. Recent developments in high-fidelity PES fitting to highly accurate *ab initio* data have enabled reliable quantum and quasi-classical studies of collisional dynamics involving polyatomic molecules.[21,30] However, developing accurate high-dimensional PESs for complex systems remains a challenge. Collision induced energy transfer processes present a unique case, in which no chemical bond breaking/forming takes place. As a result, the exchange of atoms between the two colliding partners can be ignored. This feature allows simplifications in the development of PESs for such multi-component systems. To this end, the full interaction PES can be conveniently written as a sum of intra- and inter-molecular terms. The monomer PESs are of significantly lower dimensionality and often available. The intermolecular term thus becomes the focus.

Recent theoretical studies of energy transfer dynamics have showed that the intermolecular PES expressed in terms of a pairwise sum could introduce significant errors. As a result, it is highly desirable to develop accurate non-pairwise forms of intermolecular PESs. In this work, we examine three different ways to construct the interaction PES between C_2H_2 and Ne. The benchmark is provided by a single fit of all *ab initio* data, using the PIP-NN method. The resulting 9D PES1 provides an unbiased representation of both the intra- and inter-molecular interactions in the entire configuration space. The second and third approaches express the PES as a sum of the intra- and inter-molecular terms, with the former adopted from our previous work. The intermolecular PES was fitted with two different approaches. In the first approach (PES2), the PIP method of Bowman and co-worker was used. Two different bases were used to restrict the full permutation symmetry of the PES based on physical considerations. In the second approach (PES3), the PIP-NN method is extended to fit the interaction PES. Specifically, a selected set of PIPs was used in the input layer of the NN, which enforces the necessary permutation symmetry.

All three PESs were based on fitting of ~42 000 points calculated the level of CCSD(T)-F12a/cc-pCVTZ-F12. They are all in general agreement with each other, as evidenced by small fitting errors, error distributions, as well as 1D cuts and 2D contour plots. Their validity in studying collisional energy transfer dynamics is also confirmed by preliminary QCT calculations. We conclude that PESs for dynamical studies of energy transfer can be constructed efficiently and accurately by PIP-NN fitting of both intra- and inter-molecular parts.

ACKNOWLEDGMENTS

This work was supported by the Hundred-Talent Foundation of Chongqing University (Project No. 0220001104420) and National Natural Science Foundation (No. 21573027) of China to J.L., and by US DOE (No. DE-FG02-05ER15694) to H.G. Professor Joel Bowman is thanked for sending us the script to speed up the calculations of PIPs.

[1]D. C. Tardy and B. S. Rabinovitch, Chem. Rev. **77**, 369 (1977).
[2]I. Oref and D. C. Tardy, Chem. Rev. **90**, 1407 (1990).
[3]J. R. Barker and D. M. Golden, Chem. Rev. **103**, 4577 (2003).
[4]G. W. Flynn, C. S. Parmenter, and A. M. Wodtke, J. Phys. Chem. **100**, 12817 (1996).
[5]A. W. Jasper, K. M. Pelzer, J. A. Miller, E. Kamarchik, L. B. Harding, and S. J. Klippenstein, Science **346**, 1212 (2014).
[6]A. W. Jasper, J. A. Miller, and S. J. Klippenstein, J. Phys. Chem. A **117**, 12243 (2013).
[7]R. Conte, P. L. Houston, and J. M. Bowman, J. Phys. Chem. A **117**, 14028 (2013).
[8]W. L. Hase, K. Song, and M. S. Gordon, Comput. Sci. Eng. **5**, 36 (2003).
[9]G. Lendvay and G. C. Schatz, J. Phys. Chem. **95**, 8748 (1991).
[10]T. Lenzer, K. Luther, J. Troe, R. G. Gilbert, and K. F. Lim, J. Chem. Phys. **103**, 626 (1995).
[11]Z. Li, R. Sansom, S. Bonella, D. F. Coker, and A. S. Mullin, J. Phys. Chem. A **109**, 7657 (2005).
[12]N. Sathyamurthy and L. M. Raff, J. Chem. Phys. **63**, 464 (1975).
[13]J. N. Murrell, S. Carter, S. C. Farantos, P. Huxley, and A. J. C. Varandas, *Molecular Potential Energy Functions* (Wiley, Chichester, 1984).
[14]A. J. C. Varandas, Adv. Chem. Phys. **74**, 255 (1988).
[15]T. Hollebeek, T.-S. Ho, and H. Rabitz, Annu. Rev. Phys. Chem. **50**, 537 (1999).
[16]J. Ischtwan and M. A. Collins, J. Chem. Phys. **100**, 8080 (1994).
[17]M. A. Collins, Theor. Chem. Acc. **108**, 313 (2002).
[18]R. Dawes, D. L. Thompson, A. F. Wagner, and M. Minkoff, J. Chem. Phys. **128**, 084107 (2008).
[19]R. Dawes, D. L. Thompson, A. F. Wagner, and M. Minkoff, J. Phys. Chem. A **113**, 4709 (2009).
[20]B. J. Braams and J. M. Bowman, Int. Rev. Phys. Chem. **28**, 577 (2009).
[21]J. M. Bowman, G. Czakó, and B. Fu, Phys. Chem. Chem. Phys. **13**, 8094 (2011).
[22]C. M. Handley and P. L. A. Popelier, J. Phys. Chem. A **114**, 3371 (2010).
[23]J. Behler, Phys. Chem. Chem. Phys. **13**, 17930 (2011).

[24]L. M. Raff, R. Komanduri, M. Hagan, and S. T. S. Bukkapatnam, *Neural Networks in Chemical Reaction Dynamics* (Oxford University Press, Oxford, 2012).
[25]B. Jiang and H. Guo, J. Chem. Phys. **139**, 054112 (2013).
[26]J. Li, B. Jiang, and H. Guo, J. Chem. Phys. **139**, 204103 (2013).
[27]J. Li and H. Guo, Phys. Chem. Chem. Phys. **16**, 6753 (2014).
[28]J. Li, S. Carter, J. M. Bowman, R. Dawes, D. Xie, and H. Guo, J. Phys. Chem. Lett. **5**, 2364 (2014).
[29]J. Li, J. Chen, Z. Zhao, D. Xie, D. H. Zhang, and H. Guo, J. Chem. Phys. **142**, 204302 (2015).
[30]J. Li, B. Jiang, H. Song, J. Ma, B. Zhao, R. Dawes, and H. Guo, J. Phys. Chem. A **119**, 4667 (2015).
[31]T. Lenzer and K. Luther, J. Chem. Phys. **105**, 10944 (1996).
[32]A. W. Jasper and J. A. Miller, J. Phys. Chem. A **113**, 5612 (2009).
[33]F. Pirani, S. Brizi, L. F. Roncaratti, P. Casavecchia, D. Cappelletti, and F. Vecchiocattivi, Phys. Chem. Chem. Phys. **10**, 5489 (2008).
[34]R. A. Buckingham, Proc. R. Soc. London, Ser. A **168**, 264 (1938).
[35]A. J. C. Varandas and S. P. J. Rodrigues, J. Chem. Phys. **106**, 9647 (1997).
[36]S. P. J. Rodrigues and A. J. C. Varandas, J. Phys. Chem. A **102**, 6266 (1998).
[37]K. T. Tang and J. P. Toennies, J. Chem. Phys. **80**, 3726 (1984).
[38]A. W. Jasper and J. A. Miller, J. Phys. Chem. A **115**, 6438 (2011).
[39]A. Shank, Y. Wang, A. Kaledin, B. J. Braams, and J. M. Bowman, J. Chem. Phys. **130**, 144314 (2009).
[40]Y. Wang, B. C. Shepler, B. J. Braams, and J. M. Bowman, J. Chem. Phys. **131**, 054511 (2009).
[41]J. S. Mancini and J. M. Bowman, J. Chem. Phys. **139**, 164115 (2013).
[42]J. S. Mancini and J. M. Bowman, J. Phys. Chem. A **118**, 7367 (2014).
[43]J. S. Mancini and J. M. Bowman, J. Phys. Chem. Lett. **5**, 2247 (2014).
[44]Y. Paukku, K. R. Yang, Z. Varga, and D. G. Truhlar, J. Chem. Phys. **139**, 044309 (2013).
[45]R. Conte, C. Qu, and J. M. Bowman, J. Chem. Theory Comput. **11**, 1631 (2015).
[46]R. Conte, P. L. Houston, and J. M. Bowman, J. Chem. Phys. **140**, 151101 (2014).
[47]C. Qu, R. Conte, P. L. Houston, and J. M. Bowman, Phys. Chem. Chem. Phys. **17**, 8172 (2015).
[48]M. Nikow, M. J. Wilhelm, J. M. Smith, and H.-L. Dai, Phys. Chem. Chem. Phys. **12**, 2915 (2010).
[49]J. M. Smith, M. Nikow, J. Ma, M. J. Wilhelm, Y.-C. Han, A. R. Sharma, J. M. Bowman, and H.-L. Dai, J. Am. Chem. Soc. **136**, 1682 (2014).
[50]H. Han, A. Li, and H. Guo, J. Chem. Phys. **141**, 244312 (2014).
[51]L. Guo, H. Han, J. Ma, and H. Guo, J. Phys. Chem. A **119**, 8488 (2015).
[52]T. B. Adler, G. Knizia, and H.-J. Werner, J. Chem. Phys. **127**, 221106 (2007).
[53]G. Knizia, T. B. Adler, and H.-J. Werner, J. Chem. Phys. **130**, 054104 (2009).
[54]J. G. Hill, S. Mazumder, and K. A. Peterson, J. Chem. Phys. **132**, 054108 (2010).
[55]H.-J. Werner, P. J. Knowles, G. Knizia, F. R. Manby, M. Schütz *et al.*, MOLPRO, version 2010.1, a package of *ab initio* programs, 2010, see http://www.molpro.net.
[56]S. F. Boys and F. Bernardi, Mol. Phys. **19**, 553 (1970).
[57]X. Hu, W. L. Hase, and T. Pirraglia, J. Comput. Chem. **12**, 1014 (1991).
[58]W. L. Hase and D. G. Buckowski, Chem. Phys. Lett. **74**, 284 (1980).